Structural Stabilization of [2Fe-2S] Ferredoxin from *Halobacterium salinarum*

Amal K. Bandyopadhyay, G. Krishnamoorthy,* and Haripalsingh M. Sonawat*

Department of Chemical Sciences, Tata Institute of Fundamental Research, Homi Bhabha Road, Mumbai 400 005, India

Received July 12, 2000; Revised Manuscript Received November 21, 2000

ABSTRACT: The ferredoxin of the extreme haloarchaeon *Halobacterium salinarum* requires high (>2 M) concentration of salt for its stability. We have used a variety of spectroscopic probes for identifying the structural elements which necessitate the presence of high salt for its stability. Titration of either the fluorescence intensity of the tryptophan residues or the circular dichroism (CD) at 217 nm with salt has identified a structural form at low (<0.1 M) concentration of salt. This structural form (L) exhibits increased solvent exposure of W side chain(s) and decreased level of secondary structure compared to the native (N) protein at high concentrations of salt. The L-form, however, contains significantly higher levels of both secondary and tertiary structures compared to the form (U) found in highly denaturing conditions such as 8 M urea. The structural integrity of the L-form was highly pH dependent while that of N- or U-form was not. The pH dependence of either fluorescence intensity or CD of the L-form showed the presence of two apparent p*K* values: ∼5 and ∼10. The structural integrity of the L-form at low (<5) pH was very similar to that of the N-form. However, titration with denaturants showed that the low pH L-form is significantly less stable than the N-form. The increased destabilization of the L-form with the increase in pH was interpreted to be due to mutual Coulombic repulsion of carboxylate side chains (p*K* ≈ 6) and due to the disruption of salt bridge(s) between ionized carboxylates and protonated amino groups (p*K* ≈ 10). Estimation of solvent accessibility of W residues by fluorescence quenching, and measurement of decay kinetics of fluorescence intensity and anisotropy strongly support the above model. Polylysine interacted stoichiometrically with the L-form of ferredoxin resulting in nativelike structure. In conclusion, our studies show that high concentration of salt stabilizes the haloarchaeal ferredoxin in two ways: (i) neutralization of Coulombic repulsion among carboxyl groups of the acidic residues, and (ii) salting out of hydrophobic residues leading to their burial and stronger interaction.

The structure, conformational stability, dynamics, and function of globular proteins are controlled by the solvent (*1*−*8*). The extreme effectiveness of this control is exemplified by the proteins found in the organisms which have evolved in extreme environmental conditions such as in high salt (*9*, *10*), acidic (*11*), alkaline (*12*), temperature (*13*, *14*), and pressure (*15*, *16*) environment. For example, soluble proteins from halophilic organisms are expected to have structural features which require high concentration of salt for stabilization and function of the protein. Molecular understanding of the selectiveness by which the halophilic proteins are stabilized by high concentrations of salt would be useful in delineating the rules which govern the stability of the protein in general.

Halophilic proteins, in general, have been reported to have a higher molar excess of acidic amino acids, fewer basic residues, and a higher number of small hydrophobic residues than the corresponding nonhalophilic proteins (*17*, *18*). This is especially so for the soluble proteins from the extreme halophiles. They are characterized by their conformational stability and are optimally functional at salt concentrations in excess of 2 M NaCl (*19*−*21*). Crystal structures of two halophilic proteins, namely, halophilic malate dehydrogenase (*22*) and ferredoxin (*23*) from *Haloarcula marismortui* show clusters of the negatively charged amino acids on the protein surface (Figure 1). The former is stabilized by specific network of hydrated salt ions (*24*−*28*) and increased number of salt bridges (*22*), while the latter shows tightly bound water molecules (*23*). A moderately halophilic protein, dihydrofolate reductase of *Haloferax volcanii*, on the other hand, does not possess a significantly higher molar excess of negatively charged amino acid residues in comparison to the nonhalophilic DHFR. This protein is stable at concentration of >0.5 M NaCl and exhibits clusters of noninteracting negatively charged residues on its surface (*29*).

Ferredoxin from the extreme halophilic *Halobacterium salinarum* (*Hs*Fd)[1] is one of the ideal candidates for which some of the basic questions on protein stability could be addressed. *Hs*Fd is a small single subunit protein of 128 amino acids. It has two tryptophan side chains (W16 and W59), no disulfide bonds, and a [2Fe-2S] chromophore (*30*−

* To whom correspondence should be addressed. Phone: +91-22-2152971 ext. 2377. Fax: +91-22-2152110. E-mail:hms@mailhost.tifr.res.in.

[1] Abbreviations: CAPS, 3-[cyclohexylamino]-1-propanesulfonic acid; CAPSO, 3-[cyclohexylamino]-2-hydroxy-1-propanesulfonic acid; MES, 2-[*N*-morpholino]ethansulfonic acid; MOPS, 3-[*N*-morpholino]propanesulfonic acid; NATA, *N*-acetyl-L-tryptophanamide; *Hm*Fd, Ferredoxin from *Haloarcula marismortui*; HmMDH, malate dehydrogenase from *Haloarcula marismortui*; *Hs*Fd, Ferredoxin from *Halobacterium salinarum* N, native form of *Hs*Fd at high (>4 M) concentration of salt; L, low (<0.1M) salt form; U, unfolded form in the presence of 8 M urea; PL, polylysine bound form at low (<0.1 M) salt.

10.1021/bi001614j CCC: $20.00
Published on Web 01/10/2001

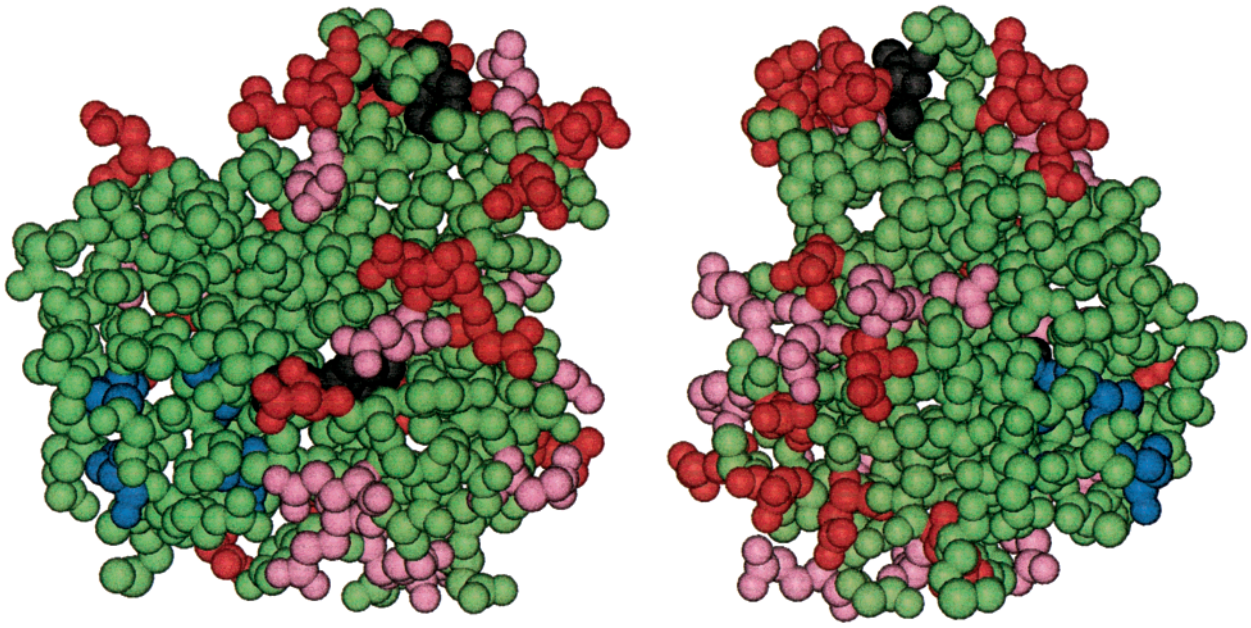

FIGURE 1: Space filling model of the ferredoxin of *Haloarcula marismortui* (*23*). Note the clusters of negatively charged residues, aspartate (red) and glutamate (pink) on the surface. The tryptophan and cysteine residues are shown in black and blue, respectively. Two views of the protein are presented.

32). Further, nearly one-third of its amino acids is either aspartic acid or glutamic acid, similar to many other halophilic proteins (*33*). This provides a clue to the requirement of high salt concentrations for their stability. We had earlier reported on the salt-dependent stability of the tertiary and secondary structure and the integrity of its [2Fe-2S] center (*34*). Does the absence of high concentrations of salt destabilize local structure(s) or the entire structure? Destabilization of the local structure(s) alone would result in partially folded overall structure which would also be relevant in understanding the mechanisms of folding. With this view, we have studied, by using fluorescence and CD spectroscopy, the various structural forms of the ferredoxin from the extreme haloarchaeon *H. salinarum* under a variety of conditions. We have also found novel conditions for stabilizing the structure in low concentration of salt.

MATERIALS AND METHODS

Purification and characterization of *Hs*Fd were performed by the method reported earlier (*34*). The concentration of ferredoxin was determined spectrophotometrically using ϵ_{420} of 10 000 M^{-1} cm^{-1}. Protein concentration used was typically 4−25 μM unless otherwise specified. MOPS, CAPSO, MES, Tris, polylysine, pentalysine, poly-glutamate, acrylamide, and CsCl were purchase from Sigma Chemical Co., and ultrapure urea was from Boeheringer Mannheim, Germany. All other reagents were analytical grade and were used as supplied.

The solutions used in the study were double filtered. All spectroscopic measurements were carried out at ambient temperature in 10 mM sodium phosphate buffer (buffer A), pH 7.3, unless mentioned otherwise. The samples were incubated at ambient temperature in the corresponding solution for a period of 35−40 h. For pH titration experiment, a cocktail buffer (buffer B) was prepared using 10 mM each of MOPS, CAPSO, MES, and Tris, and the pH of the solution was adjusted from 5.0 to 11.4 at an interval of 0.5. For pH 4.0, 4.5, and 4.75, sodium acetate buffer was used at 25 mM concentration. The ionic strength was maintained by including appropriate volume of 5 M NaCl. For salt-dependent equilibrium studies, a stock solution of 5 M NaCl in buffer A was prepared and diluted to various concentrations using the same buffer (buffer A). Concentration of salt in the equilibrium study was varied from 0.05 to 4.5 M.

A stock solution of 8 M urea was prepared in buffer A containing 4.5 M salt. Concentration of urea was varied in the range 0−8 M. To avoid the presence of cyanides, the urea solution was passed through Amberlite column and used the same day.

For polylysine, polyglutamate, and pentalysine titration experiments, stock solutions were prepared for each of the poly acids in buffer A and different concentrations were achieved by taking aliquots from the stock solution and diluting them with solution containing protein.

Equilibrium Studies in CD and Steady-State Fluorescence. All CD measurements were done on a Jasco600 spectropolarimeter. Far-UV spectra were recorded from 200 to 250 nm using 0.1 cm path-length silica quartz cell. Ten scans were accumulated per spectrum and were smoothed. All CD data are expressed as mean residue ellipticities at a given wavelength.

Steady-state fluorescence was measured using "Spex" spectrofluorimeter. The T-format fluorimeter with two detection channels help in improving the precision of fluorescence intensity ratio at two wavelengths and fluorescence anisotropy measurements. Excitation wavelength was 295 nm with slit width 2, 3, and 4 nm depending upon the requirement and protein concentration. Emission spectra were recorded from 310 to 500 nm using a 1 cm path-length quartz cell. For steady-state anisotropy measurements, each reading was an average of 10 individual readings.

Fluorescence Quenching Measurements. Measurements were made in protein having high-salt, low-salt, high salt in

8 M urea, low-salt protein treated with poly-lysine. Quenching experiments were performed using acrylamide, KI and CsCl. For iodide quenching experiments, sodium thiosulfate was added to avoid formation of I_3^-. Freshly prepared solutions of quenchers were used each day.

Stern−Volmer plots were constructed by using the variation of the fluorescence intensity at its maxima depending upon the state of the protein in the solution. Each value was volume corrected. Stern−Volmer plots were fitted to the following equation:

$$\frac{I_0}{I} = (1 + K_{SV}[Q]) \tag{1}$$

where I_0 is the fluorescence intensity of the protein in absence of quencher, I is the volume corrected fluorescence intensity of the sample in the presence of a concentration Q of quencher, K_{SV} is the Stern−Volmer constant (association constant) and could be obtained from the slope of the curve. Stern−Volmer constant is equal to $\tau_o k_q$, where k_q is the bimolecular quenching constant and τ_o is the fluorescence lifetime of the fluorophor in the absence of quencher.

Time-Resolved Fluorescence Measurements. The samples were prepared as mentioned in the steady-state experiment. Protein concentration was 25 μM for each measurement. Time-resolved fluorescence decay of ferredoxin was observed by using a CW mode-lock frequency-doubled Nd:YAG laser driven dye (Rhodamine-6G) laser operating at a repetition rate of 800 kHz with a pulse width of the order of 4−10 ps and tunability in the region of 570−640 nm (*35*). Fluorescence decay curves were obtained by using a time-correlated single-photon counting setup (*35*) coupled to a microchannel plate photomultiplier. The instrument response function (IRF) was obtained at 295 nm using a dilute colloidal suspension of dried nondairy coffee whitener. Protein was excited at 295 nm using the second harmonic output of the dye laser from an angle-tuned KDP crystal, and the fluorescence emission was collected through a 320 nm cutoff filter followed by a monochromator. The peak counts obtained in control experiments were comparable to the background level. In fluorescence lifetime measurements, emission was monitored at magic angle (54.7°) to eliminate the contribution from the decay of anisotropy.

Time-Resolved Data Analysis. Time-resolved anisotropy [r(t)] was calculated using the following formula:

$$r(t) = \frac{I_\Pi - I_\perp G(\lambda)}{I_\Pi + 2I_\perp G(\lambda)} \tag{2}$$

where I_Π and $I_\perp$ are the emissions in the directions parallel and perpendicular to the polarization of the excitation beam. $G_{(\lambda)}$ is the geometry factor at the wavelength of the emission.

Fluorescence decay curves at the magic angle were analyzed by deconvolution of the observed decay with the IRF to obtain the intensity decay function represented as a sum of three exponentials:

$$I(t) = \sum_i \alpha_i \exp(-t/\tau_i), \qquad i = 1-3 \tag{3}$$

where I(t) is the fluorescence intensity at time t and α_i is the amplitude of the ith lifetime such that $\sum\alpha_i = 1$.

Time-resolved anisotropic decay was analyzed based on the model

$$I_\Pi(t) = \frac{I}{3} I(t)[1 + 2r(t)] \tag{4}$$

$$I_\perp(t) = \frac{I}{3} I(t)[1 - r(t)] \tag{5}$$

$$r(t) = r_0 \sum_i \beta_i \exp(-t/\tau_{r_i}), \qquad i = 1 \text{ or } 2 \tag{6}$$

where r_0 is the initial anisotropy, β_i is the amplitude of the ith rotational correlation time τ_{r_i} such that $\sum_i \beta_i = 1$. In cases where the decay of $r(t)$ was biexponential, τ_{r_1} and τ_{r_2} represent the internal rotation of tryptophan (W) residues and the overall tumbling of the protein, respectively. In the present model, each τ_{r_i} is associated with both τ_{r_1} and τ_{r_2}. Nonlinear least-squares analysis was performed to extract the amplitude parameters α_i, β_i, lifetimes τ_i and correlation times τ_{r_i} (*36*). In the case of time-resolved anisotropy decay, I_Π and $I_\perp$ were analyzed globally (*37*) by using the measured IRF. Since the goodness of fit were satisfactory with two correlation times (τ_{r_1} and τ_{r_2}), we have not increased the number of τ_{r_i} components to more than two.

All the time-resolved measurements involving systematic variation of a specific experimental condition were carried out on the same day. Since the analysis of time-resolved anisotropy decay involves multiparameter fitting with several unknowns, the values obtained were employed to calculate steady-state anisotropy (r_{SS}).

$$r_{SS} = \frac{r_0 \sum_i \sum_j \alpha_i \beta_j \left[\frac{1}{\tau_i} + \frac{1}{\tau_{rj}}\right]^{-1}}{\sum_i \alpha_i \tau_i} \tag{7}$$

This value was compared with the experimentally obtained value of the steady-state anisotropy at the same excitation and emission wavelengths under identical conditions. Only the set of parameters which gave the computed steady-state anisotropy value close to the observed value was accepted.

RESULTS

Fluorescence Intensity and CD Observations. The fluorescence emission spectrum due to W16 and W59 of *Hs*Fd was very sensitive to the concentration of salt (Figure 2). The emission maximum shifted from ∼355 nm to ∼335 nm when the salt concentration was increased from 0.05 to 4.5 M. Comparison of these spectra with that of NATA, a model compound for tryptophan (Figure 2), shows that either one or both of the tryptophans get exposed to the solvent when the salt concentration was reduced from 4.5 to 0.05 M. The spectra recorded under rigorously controlled anaerobic conditions (not shown) were similar to those presented in Figure 2. Therefore, all the experiments reported here were performed under ambient conditions. Figure 3 shows salt concentration dependence of the ratio (F_{360}:F_{330}) of fluorescence intensities at 360 nm (F_{360}) and 330 nm (F_{330}). The F_{360}:F_{330} shows an apparent monotonic transition between two states. Since the ratio of the intensities does not depend

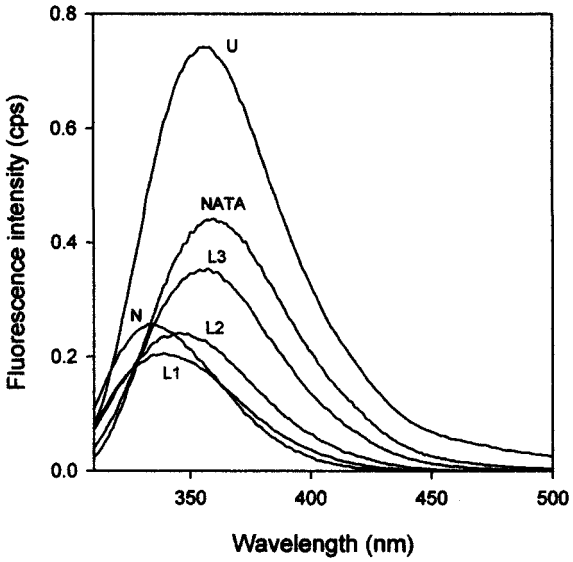

FIGURE 2: Fluorescence emission spectra of native (N), U-form (U), and L-forms at 1 M (L1), 0.2 M (L2), and 0.05 M (L3) NaCl concentrations of ferredoxin from *Halobacterium salinarum.* The emission spectra of the model compound NATA has been presented for comparison.

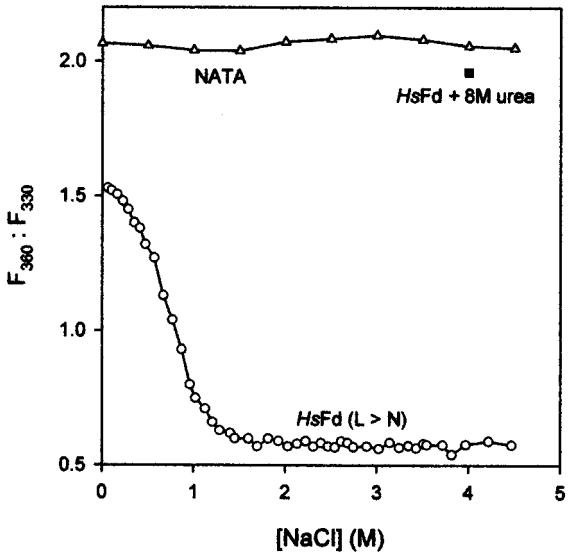

FIGURE 3: Equilibrium refolding titration of ferredoxin from *Halobacterium salinarum* as a function of NaCl concentration followed by tryptophan fluorescence. Salt dependence of NATA presented as a reference. Equilibrium unfolding of native *Hs*Fd in the presence of 8 M urea has been presented as a single point. Other experimental conditions are similar as mentioned in the Materials and Methods.

on the concentration of the protein but only upon its structural constituents, the ratio was used throughout the present work unless required otherwise. The ratio F_{360}:F_{330} decreased from 1.55 to 0.6 when the salt concentration was increased from 0.05 to 4.5 M. The intensity ratio of NATA was largely insensitive to the salt concentration, as expected.

To check whether the change in the structure of *Hs*Fd (Figure 2) at low salt concentration (L-form) is due to either local perturbation or complete denaturation of the protein, comparison was made with the protein denatured by 8 M urea (U-form). The fluorescence emission characteristics (Figure 2) and the intensity ratio (Figure 3) of the U-form are closer to those of NATA than to the L-form. It is likely

Table 1

(A) Bimolecular Rate Constant (k_q) for the Quenching of Fluorescence of the Different Forms of the Ferredoxin of *H. salinarum*

	$k_q \times 10^9$ ($M^{-1}s^{-1}$)		
form of *Hs*Fd	iodide	cesium chloride	acrylamide
N	1.00	0.99	2.60
L	1.61	1.16	6.30
U	1.62	1.16	6.10
PL	1.01	0.99	2.30

(B) Bimolecular Rate Constant (k_q) for Quenching of Fluorescence of N- and L-Forms of the Ferredoxin of *H. salinarum* at Different pH Using KI and Acrylamide

	$k_q \times 10^9$ ($M^{-1}s^{-1}$)			
	N-form		L-form	
pH	acrylamide	iodide	acrylamide	iodide
4.5	2.61	1.04	3.56	1.16
5.0	2.67	1.07	4.58	1.30
7.0	2.60	1.04	6.07	1.56
9.0	2.71	1.09	6.47	1.60

that the L-form is partially structured compared to the U-form. This was further tested by quenching of fluorescence by either acrylamide (Ac), iodide (I^-), and cesium (Cs^+). Accessibility to these quenchers is a good indicator of solvent exposure of tryptophan (*38*, *39*). The bimolecular quenching constant k_q derived from the Stern−Volmer plots (data not shown) are presented in Table 1A. Several points are noteworthy in these data. First, the k_q of the U-form is larger than that of the native N-form suggesting, as expected, a higher accessibility of the W side chains when the protein is denatured. Second, the similar value of k_q obtained for the L- and U-forms indicates similar solvent accessibility of the W side chains in the two forms. Third, similar values of k_q for the N-form with both the ionic quenchers (I^- and Cs^+) indicate that the k_q reflect the true solvent accessibility unaltered by any electrostatic interaction of the ionic quenchers with the charged side chains near the tryptophans.

Far-UV circular dichroism (CD) spectra indicate global structural characteristics of proteins whereas tryptophan fluorescence might be restricted to local changes in some cases. Figure 4 shows typical CD spectra of the different forms of *Hs*Fd. It is clear that the L-form is between the N- and U-form. This, along with the fluorescence measurements, indicates that L-form has a residual level of secondary as well as tertiary structure.

How compact is the L-form? The equilibrium transition curves for urea-induced unfolding of *Hs*Fd monitored by fluorescence are presented in Figure 5. The transition curves (Figure 3 and 5) suggest that the L→U transition may not be cooperative unlike the transition N→L (Figure 3) or N→U (Figure 5). The midpoint of L→U transition is at a concentration of ∼1.0M urea while that of N→U transition occurs at ∼4.7 M urea indicating thereby that the L-form is less compact than the N-form.

To explore the origin of the structural changes attributed to the L-form, the F_{360}:F_{330} and ellipticity at 217 nm were monitored for the protein at different pH values. The results are presented in Figure 6. The pH-dependent variation was observed only for the L-form and not for the N-form or, as expected, for NATA. The k_q of the N- and L-form at various

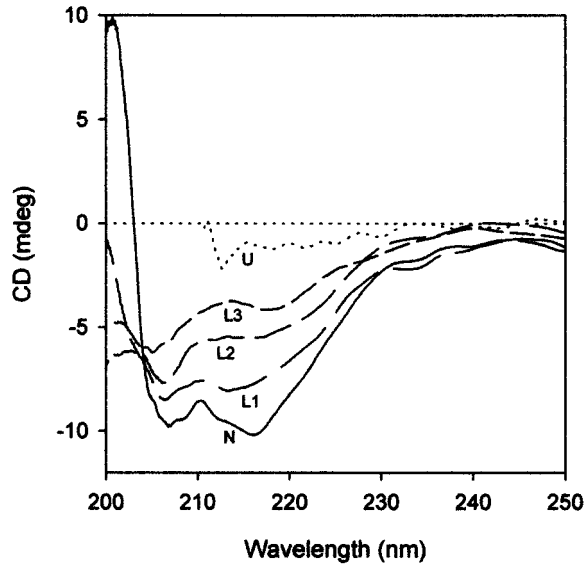

FIGURE 4: Far-UV CD spectra of native (N), L-form (L1 at 1 M NaCl, L2 at 0.2 M NaCl and L3 at 0.05 M NaCl concentration), and U-form of ferredoxin from *Halobacterium salinarum*.

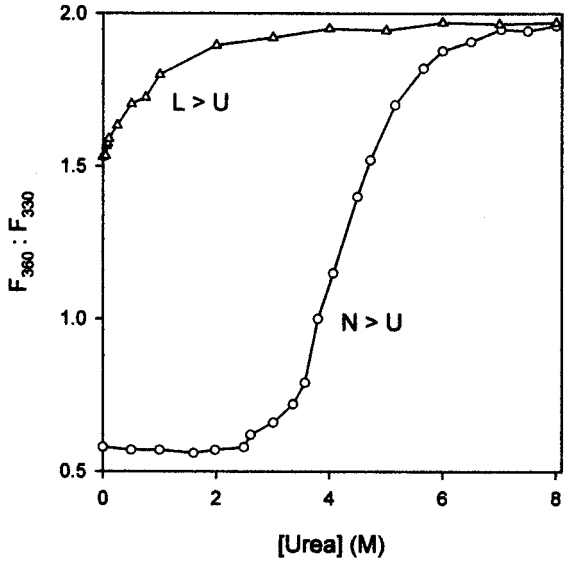

FIGURE 5: Urea-induced equilibrium unfolding transition monitored by fluorescence intensity ratio (F_{360}:F_{330}) for L-form and N-form (pH 7.3).

pH values have been listed in Table 1B. The L-form shows pH dependence whereas the N-form is independent of pH, similar to the observation made in fluorescence and CD (Figure 6). At low pH, the L-form exhibited parameters that approached toward those of the N-form. This suggests that the structure of L-form is similar to that of N-form at pH <5. The pH titration curves (Figure 6) show two apparent p*K* values, one at ~6 and another at ~10. Does the similarity of spectral parameters of the L-form and N-form observed below pH 5.0 imply the similarity of their structure? Figure 7 shows equilibrium urea-induced unfolding of the L- and N-form at pH 4.5 as monitored by F_{360}:F_{330}. The apparent midpoints of transition for the L- and N-form are 1.6 and 4.6 M urea, respectively.

Can the effects of ionization of the carboxylates and the resultant spectral changes (Figure 6) be contained by any means other than the high salt concentration? Specifically,

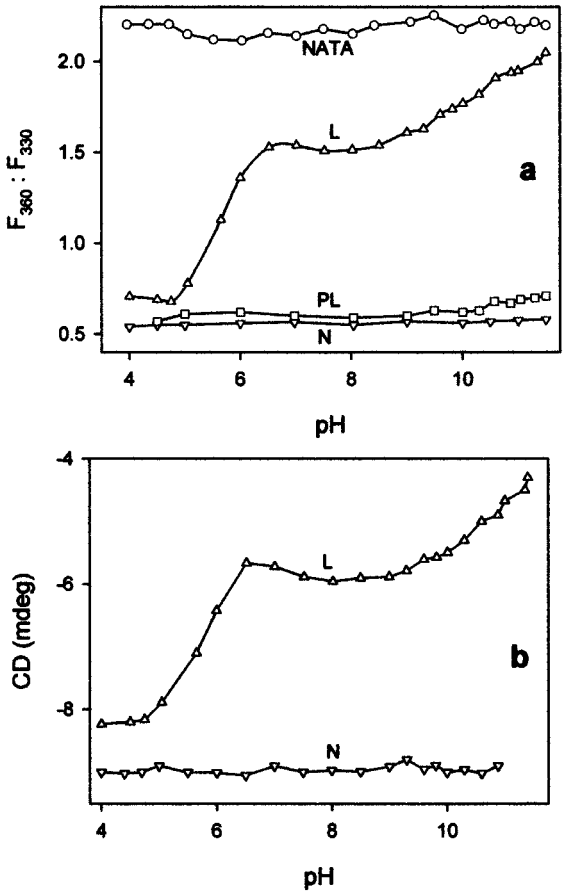

FIGURE 6: pH dependence of various forms of ferredoxin from *Halobacterium salinarum* as measured by (a) fluorescence intensity ratio (F_{360}:F_{330}) and (b) far-UV CD ellipicity at 217 nm.

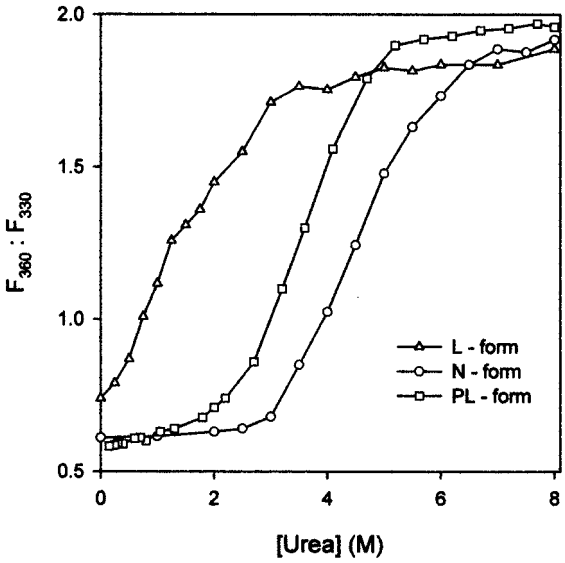

FIGURE 7: Urea induced equilibrium unfolding transition of ferredoxin from *Halobacterium salinarum* measured by fluorescence intensity ratio (F_{360}:F_{330}). L-form (0.05 M NaCl in 10 mM sodium acetate buffer, pH 4.5), N-form (4.5 M NaCl in 10 mM sodium acetate buffer pH 4.5) and PL-form (2.5 mM sodium phosphate buffer pH 8.0, 0.05 M NaCl and 1:1::*Hs*Fd:polylysine). After addition of urea, the solutions were incubated at ambient temperature for 30 h.

can one revert the L-form into N-form by any agent other than salt? The effect of polylysine and polyglutamic acid on the spectral characteristics of the protein was examined.

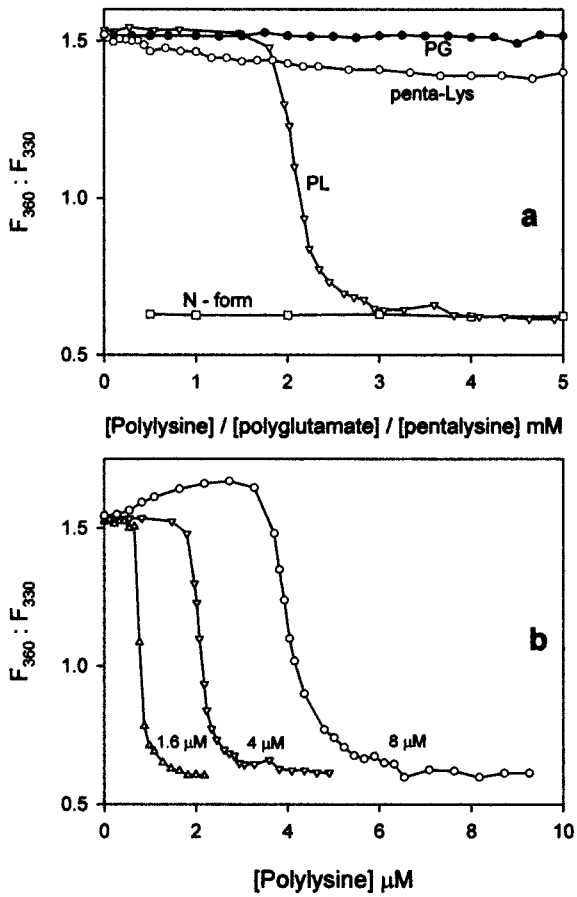

FIGURE 8: Equilibrium titrations of L-form of ferredoxin from *Halobacterium salinarum* as a function of (a) polyglutamate (PG), pentalysine (penta-PL), polylysine (PL) concentration. The *Hs*Fd was 4 μM in 2.5 mM sodium phosphate buffer, pH 8.0 containing 0.05 M NaCl. Similar titration of the N-form (4.5 M NaCl) of ferredoxin as a function of polylysine is presented for comparison. (b) The indicated concentration of the protein in the same buffer was titrated with polylysine.

Figure 8a shows the F_{360}:F_{330} of the L-form of *Hs*Fd titrated with polylysine, polyglutamic acid and pentalysine. Of the three, polylysine exhibited the most striking effect. Its addition to the L-form of HsFd changed F_{360}:F_{330} from 1.5 to 0.6, similar to the N-form. Further, the effect was stoichiometric with respect to the concentration of protein (Figure 8b). Higher concentrations of *Hs*Fd required higher levels of polylysine for changing the F_{360}:F_{330}. Polylysine did not significantly affect the native protein in high salt concentration (Figure 8a). Thus these data show that polylysine can indeed affect the transition of *Hs*Fd from the L-form to a state almost similar to the N-form. We shall call this form as PL-form.

For further characterization of the PL-form we measured the accessibility of its tryptophans by fluorescence quenching, as before. The value of k_q (Table 1A) for the PL-form is similar to that of the N-form. The midpoint of denaturation of the PL-form by urea is observed at ~4.0 M urea, a value higher than the L-form but lower than the N-form (Figure 7).

Fluorescence Anisotropy Studies. The dynamics of the various structural forms of *Hs*Fd was also examined by steady-state fluorescence anisotropy (r_{SS}) of W16 and W59. Table 2 lists the value of r_{SS} obtained under various conditions. The r_{SS} of the L-form is intermediate of the values of the N- and the U-forms and at pH 7.0, it is closer to that of the U-form. Further, r_{SS} of the L-form decreased from 0.118 to 0.073 when the pH was increased from 5.0 to 9.0. In contrast, both the N-form and the U-form did not show pH-dependent r_{SS} values. Thus these data corroborate the other observations which indicate that the L-form has a partial structure whose level is pH-dependent. The significantly higher value (0.298) of r_{SS} of the PL-form could be due to the overall increase in the hydrodynamic radius of *Hs*Fd by the binding of polylysine. However, the conclusions on the dynamics based on r_{SS} are only tentative since r_{SS} is a function of both the dynamics and fluorescence decay kinetics.

Table 2: Steady-State Fluorescence Anisotropy of the Ferredoxin of *H. salinarum*

	anisotropy (r_{ss})			
pH	N	L	U	PL
5.0	0.144 ± 0.005	0.118 ± 0.002	0.068 ± 0.003	nd[a]
5.5	0.145 ± 0.003	0.102 ± 0.003	nd	nd
6.0	0.144 ± 0.001	0.087 ± 0.003	nd	nd
6.5	0.144 ± 0.004	0.079 ± 0.003	nd	nd
7.0	0.145 ± 0.002	0.77 ± 0.001	0.068 ± 0.002	0.298 ± 0.004
7.5	0.145 ± 0.002	0.074 ± 0.003	nd	nd
8.0	0.153 ± 0.003	0.075 ± 0.002	nd	nd
8.5	0.144 ± 0.002	0.072 ± 0.003	nd	nd
9.0	0.144 ± 0.002	0.074 ± 0.003	0.067 ± 0.002	nd

[a] nd, not determined.

Table 3: Parameters Obtained from Time-Resolved Fluorescence Measurements of the Ferredoxin of *H. salinarum*

HsFd		fluorescence lifetime (ns)			amplitude				
form	pH	τ_1	τ_2	τ_3	α_1	α_2	α_3	$\tau_m = \Sigma\alpha_i\tau_i$	χ^2_{red}
N	5.0	4.58	1.20	0.62	0.07	0.32	0.61	1.10	1.03
	7.0	4.95	1.10	0.63	0.05	0.33	0.62	1.09	1.12
	9.0	4.80	1.16	0.64	0.06	0.31	0.63	1.03	0.89
L	5.0	3.60	1.28	0.36	0.12	0.46	0.42	1.20	1.13
	7.0	3.40	1.50	0.44	0.20	0.40	0.40	1.50	0.99
	9.0	3.60	1.30	0.40	0.15	0.42	0.43	1.56	0.99
U	7.0	4.2	1.65	0.45	0.35	0.40	0.25	2.45	1.09
PL	8.0	4.8	1.24	0.75	0.03	0.15	0.82	0.94	1.30

Decay Kinetics of Fluorescence Intensity and Anisotropy. Although controversial, time-resolved fluorescence of tryptophan(s) has rendered useful information for numerous proteins (*40*). Decay of fluorescence intensity of the tryptophan residues in *Hs*Fd followed a sum of three exponentials (Table 3). The mean lifetime (τ_m) for different forms of *Hs*Fd is also presented in Table 3. The τ_m of the L-form increases with increasing pH, whereas that of the N-form was independent of pH. Moreover, the PL- and N-form exhibited similar values of τ_m.

Rotational dynamics of tryptophan side chains has been effectively used in probing the level of structural integrity in proteins (*41*). The overall kinetics of fluorescence depolarization of both the tryptophan side chains in the *Hs*Fd was analyzed by a sum of exponentials. The values of rotational correlation time (τ_r) were ~0.1 and ~6 ns for the N-state (Table 4). In the L-form, the shorter τ_r was in the range 0.1−0.2 ns and the longer τ_r in the range 1.0−2.5 ns. While the shorter τ_r was not sensitive to pH, the longer τ_r decreased from ~2.5 to ~1.3 ns when the pH was raised from 5 to 11. Thus, the L-form at higher pH values was

Table 4: Parameters Associated with the Decay of Fluorescence Anisotropy of the Ferredoxin of *H. salinarum*

HsFd form	pH	r_0[a]	τ_{r1}[b] (ns)	τ_{r2}[b] (ns)	β_1[c]	β_2[c]	χ^2_{red}
N	5.0	0.24	0.11	6.1	0.60	0.40	1.73
	7.0	0.23	0.15	6.7	0.58	0.42	1.61
	9.0	0.23	0.09	5.6	0.59	0.41	1.48
L	4.5	0.29	0.20	2.6	0.53	0.47	1.58
	7.0	0.30	0.18	1.9	0.51	0.49	1.36
	9.0	0.27	0.19	1.7	0.48	0.52	1.66
	11.0	0.28	0.17	1.3	0.44	0.56	1.56
PL	7.5	0.30	0.10	9.5	0.36	0.64	2.80
U	7.0	0.27	0.15	1.4	0.50	0.50	1.70

[a] Intial anisotropy. [b] Rotational correlation time. [c] Amplitudes such that $\Sigma\beta_i = 1$.

very similar to the U-form whose τ_r values were ~0.15 and 1.4 ns. In the polylysine bound state (PL-form) the protein showed τ_r values of 0.1 and 9.5 ns.

DISCUSSION

The adaptation of proteins to extreme environments such as extreme of salinity, pH, temperature, and hydrostatic pressure (*12*) could involve more than one strategy. Even for the proteins from the same species of extreme halophile, e.g., *Halobacterium cutirubrum*, a wide spectrum of adaptation modes with respect to its maximal activity and stability is seen (*19*). Similarly, crystal structures of *Hm*MDH and *Hm*Fd from *Haloarcula marismortui* also showed variation in their adaptation process. Excess surface negative charges along with **a** greater number of salt bridges in the former and tighter binding of water molecules along with the N-terminal extra segment in the latter were thought to be the reason for their adaptation in the supersaturated saline environments (*22*, *23*). Homology-based modeling study of halophilic glutamate dehydrogenase showed that with fewer surface lysine residues the hydrophobic interactions on the protein surface were considerably reduced which contributes significantly to the halophilic adaptation (*43*). The halophilic protein studied here is a single subunit protein, *Hs*Fd. It has 88% homology with *Hm*Fd and is well suited for studying the mechanism by which the protein is stabilized at high concentration of salt and understanding the cause of instability in low-salt conditions. Baxter (*44*) suggested that the stability of halophilic proteins in high salt is due to electrostatic screening of mutually repelling negative charges of the acidic amino acid residues. However, this has been inadequate in explaining the requirement of very high (>0.4 M) concentration of salt for conferring stability. Salting out of some segments of polypeptide leading to increased hydrophobic interaction perhaps necessitates multimolar concentrations of salt (*19*). Analysis of the structural features of *Hs*Fd observed under a variety of conditions at two extremes of salt concentrations namely at very high (~4.5 M) and at very low (~0.05 M), suggest the earlier electrostatic screening model as the major cause of stabilization in moderately high salt concentration. In very high salt concentrations, other stabilizing factors such as hydrophobic effects (*19*, *45*, *46*) are also involved (see below) in the stability of *Hs*Fd.

Tryptophan fluorescence is a useful indicator of structural intactness of *Hs*Fd. W16 of the protein is close to one of the clusters of negative charges (namely D12-D13-N14-G15-W16-D17-M18-D19-D20-D21-D22) and, therefore, would monitor the salt-induced structural changes. The fluorescence of W59 would be highly quenched because of its nearness to [2Fe-2S] center. The stability of the [2Fe-2S] chromophore is affected by unfolding of the protein (*34*). The contention that the observed fluorescence is largely due to W16 is supported by the linear Stern−Volmer plots of quenching of fluorescence by Ac, I^-, and Cs^+ (not shown). The crystal structure of *Hm*Fd (*23*), 88% homologous to *Hs*Fd, shows that W16 is exposed to the solvent more than W59. This is true for the high-salt native N-form. The increase in fluorescence of the L-form with increase in pH (>5) suggests that the W59 moves away from [2Fe-2S] center. The fluorescence intensity under these conditions, therefore, has contributions from both the W16 and W59. Enhancement of fluorescence intensity, also observed in the presence of urea, therefore, seems to be a sequel to the unfolding of *Hs*Fd. This difference in solvent exposure of W16 and W59 in the N-form should have resulted in nonlinear Stern−Volmer plots as reported in other cases (*37*, *47*−*49*). Hence k_q of $\sim 1 \times 10^9$ M^{-1} s^{-1}, typical for exposed tryptophan side chains, suggests that the observed fluorescence is contributed mainly by W16 in the N-form. Further, the observation of three fluorescence lifetimes cannot be used as an indication for the number of tryptophan side chains as argued by several workers. Many proteins with single tryptophan have two or three lifetimes and their origin is still disputed (*48*, *50*−*53*). Thus, the information from W fluorescence would largely pertain to the region around W16. However, since the cluster of negatively charged residues around W16 is one of several such solvent exposed clusters (*23*), its fluorescence properties are likely to reflect the overall structural intactness of the protein.

Our experiments at different pH (Figure 6) suggest that the structures of the L- and N-form are similar at low pH. This would imply that high concentration of salt is not necessary for stabilizing *Hs*Fd below pH 5. The first pH-dependent transition (Figure 6) is due to carboxyl side chains. The mutual repulsion of these solvent exposed side chains above pH 5 would destabilize the protein, increase the F_{360}:F_{330} and decrease the CD signal. The high apparent p*K* of ~6 is not unusual, since mutually interacting carboxyl side chains exhibit high p*K* values in many situations (*29*, *54*). The second transition observed at pH 9−10 (Figure 6) could represent the loss of salt bridge(s) between carboxyl side chain and basic residues such as lysines and arginines. Such salt bridges have been detected in the crystal structure of *Hm*Fd (*23*). Above pH 9−10, the deprotonated basic residues would result in the loss of positive charge required for the formation of salt bridges. Thus the pH dependence of structural parameters suggests the following overall mechanism of structural destabilization in the L-form. At pH <5, the carboxyl groups are protonated and neutral. This leads to a structure with secondary (CD) and tertiary (F_{360}:F_{330}) characteristics very similar to the high salt N-form. When the pH is raised from 6 to 9, the carboxyl groups ionize and the mutual electrostatic repulsion destabilizes the L-form protein. However, the destabilization is not complete. The F_{360}:F_{330} is a plateau around pH 6−9 and its value remains lower (~1.6) than that of either the U-form (~1.95) or NATA (~2.1). This lack of complete destabilization could be the result of salt bridge(s) mentioned above. The loss of

these salt bridge(s) above pH 10 results in an L-form protein which is devoid of any secondary and tertiary structures. The similar k_q for the L- (pH 7.0) and U-form (Table 1a) but significantly higher fluorescence intensity for the U-form compared to the L-form (Figure 1) may appear counter intuitive. However, a plausible explanation could be that the observed fluorescence of the pH 7.0 L-form is mainly contributed by the exposed W16. The fluorescence of W59 is still partially quenched by the nearby [2Fe-2S] center. The structure around W59 is destroyed by either higher pH (>9) or by urea leading to further increase in fluorescence intensity. Our observations on the pH dependence of structural integrity of *Hs*Fd is similar to the theoretical simulations on *Hm*Fd (*54*, *55*). To the best of our knowledge, our report is the first experimental observation on the pH dependence of structural intactness of any halophilic protein.

The model described above suggests repulsive electrostatic interactions among the carboxyl side chains as the major cause of destabilization of *Hs*Fd at low salt concentration. The structure of native protein (N) is, however, not pH dependent (Figure 6). The model also implies electrostatic screening of negative charges as the major role of salt in stabilizing *Hs*Fd as proposed by Baxter (*44*) for halophilic proteins in general. Strong support for this model comes from the effect of polylysine (Figure 8). It is interesting to note that 2 μM of polylysine (MW 21 000) was able to reproduce the effect of ~2 M NaCl at a protein concentration of 1.6 μM. Possibly polylysine wraps around *Hs*Fd by forming salt bridges with the surface carboxylate clusters. The structure of PL-form is more stable than the L-form at neutral pH. The presence of the alkyl groups of polylysine on the protein surface (in the polylysine−*Hs*Fd complex) would decrease the water activity and cause further stabilization by enhancing the hydrophobic interactions (*43*, *56*) of borderline hydrophobic amino acids present in *Hs*Fd. The inability of the pentalysine to wrap around the carboxylate clusters could be the reason for its significantly reduced efficiency. Spermine, a polycation used in earlier work (*57*), requires higher concentration similar to our observations on pentalysine. The extremely high efficiency shown by polylysine (Figure 8) points toward the following two implications: (1) polycations could stabilize *Hs*Fd at concentrations much lower than that of salts, and (2) the strong affinity toward polycations and the subsequent stabilization of structure could be used in biosensor applications wherein *Hs*Fd (and other halophilic protein) could be immobilized on surfaces coated with large polycations.

Our observations seem to indicate that the structures of the low-salt L-form and high-salt N-form are similar at low pH. Are their dynamics and structural stability also similar? This is answered by the following observations. (i) Similar k_q values for the two forms at low pH, indicating that the exposure and dynamics around tryptophan side chain(s) which control the k_q values are very similar. (ii) Fluorescence depolarization kinetics showing two components, the shorter τ_{r_1} (~0.1−0.2 ns) representing the local motion of the tryptophan side chain(s) was nearly identical in both L- and N-forms, and the longer τ_{r_2} (1−6 ns), arising from a contribution of segmental and global dynamics of the entire protein (Table 4) was significantly different in the two forms. There was no segmental motion in N-form at all the pH values as shown by $\tau_{r_2} \approx 6$ ns which corresponds to the rotational dynamics of a protein of 15 000 (*42*, *58*). Furthermore, this observation indicates that *Hs*Fd exists as a monomer. This is unlike some other ferredoxins such as those from *Azotobacter vinelandii* (*59*) and *Clostridium pasteurianum* (*60*), which are homodimers. In contrast, τ_{r_2} of 1−3 ns in the L-form indicates the presence of segmental motion which decreases at low pH. However, its significant presence even at pH 4.5 ($\tau_{r_2} \approx 2.6$ ns) indicates the less compact nature of the L-form at low pH when compared to N-form. (iii) Urea induced unfolding transition of the L- and the N-form (Figure 7) at pH 4.5. The L-form has a transition midpoint, which is ~3 times less than that of the N-form under identical conditions. Thus, the L-form has far less structural stability than the N-form even at low pH. However, the structural intactness of the L-form in the pH range 4−9 is between that of the N-form and the U-form. It is interesting to note that this difference in dynamics as well as structural stability of the low-salt L-form and the high-salt N-form does not get reflected in our spectroscopic measurements either in fluorescence (F_{360}:F_{330}) or in CD (θ_{217}).

Overall, our results suggest that, at low salt in neutral pH, destabilization of *Hs*Fd is mainly guided by the Coulombic repulsion of the mutually interacting negative charges. Further destabilization occurs either by increasing the pH or by introducing chaotrophs (urea) indicating the importance of salt-bridges in structural stabilization of *Hs*Fd. Neutralization of these charges by lowering the pH increases the stability of the protein but it is far less compact and stable than the native protein thereby pointing toward a second role of salt, i.e., hydrophobic interactions (*19*, *26*, *57*, *61*), in stabilizing halophilic proteins. Similarly, comparison of the midpoint of transition of PL→U (Figure 7) with that of N→U (Figure 5) shows that PL-form is less stable than the N-form, implying the importance of the second role of salt. Although PL-form is far more stable than the L-form, polylysine cannot substitute fully, the role of high concentration of salt in stabilizing *Hs*Fd. Our experiments also highlight the salting-out effect which results in increased hydrophobic interaction among the buried segments; thus, enhancing the structural stability and reducing the segmental dynamics.

ACKNOWLEDGMENT

We are grateful to Prof. A. K. Singh, Department of Chemistry, Indian Institute of Technology, Mumbai for providing the *H. salinarum* strain M1. We thank Prof. N. Periasamy for providing us the software for analyzing fluorescence decay kinetics. A.K.B. wishes to thank Ms. Ira for her help in time-resolved experiments.

REFERENCES

1. Von Hippel, P. H., and Schleich, T. (1969) in *Structure and Stability of Biological Macromolecules* (Timasheff, S. N., and Fasman, G. D. Eds.) pp 417−574, Marcel Dekker Inc.
2. Jaenicke, R. (1987) *Prog. Biophys. Mol. Biol. 49*, 117−237.
3. Eisenberg, H., and Wachtel, E. J. (1987) *Annu. Rev. Biophys. Biophys. Chem. 16*, 69−92.
4. Zaccai, G., and Eisenberg, H. (1990) *Trends Biochem. Sci. 15*, 333−337.
5. Gregory, R. B. (1995) in *Protein-Solvent Interactions* (Gregory, R. B., Ed.) pp 191−264, Marcel Dekker, New York.
6. Parsegian, V. A., Rand, R. P., and Rau, D. C. (1995) *Methods Enzymol. 259*, 43−94.

7. Timasheff, S. N., and Arakawa, T. (1996) in *Protein structure. A practical approach* (Creighton, T. E., Ed.) pp 349−364, Oxford University Press, Oxford.
8. Israelachvilli, J., and Wennerstrom, H. (1996) *Nature 379*, 219−224.
9. Ginzburg, M., Sachs, L., and Ginzburg, B. Z. (1970) *J. Gen. Physiol. 55*, 187−207.
10. Kushner, D. J. (1978) in *Microbiol life in extreme environments* (Kushner, D. J., Ed.) pp 317−368, Academic Press, London.
11. Schwermann, B., Pfau, K., Liliensiek, B., Schleyer, M., Fischer, T., and Bakker, E. P. (1994) *Eur. J. Biochem. 226*, 981−991.
12. Jaenicke, R. (1991) *Eur. J. Biochem. 202*, 715−728.
13. Jaenicke, R., and Bohm, G. (1998) *Curr. Opin. Struct. Biol. 8*, 738−748.
14. Madigan, M. T., and Oren, A. (1999) *Curr. Opin. Microbiol. 2*, 265−269.
15. Gross, M., and Jaenicke, R. (1994) *Eur. J. Biochem. 221*, 617−630.
16. Horikoshi, K. (1998) *Curr. Opin. Microbiol. 1*, 291−295.
17. Rao, J. K., and Argos, P. (1981) *Biochemistry 20*, 6536−6543.
18. Madern, D., Pfister, C., and Zaccai, G. (1995) *Eur. J. Biochem. 230*, 1088−1095.
19. Lanyi, J. K. (1974) *Bacteriol. Rev. 38*, 272−290.
20. Eisenberg, H., Mevarech, M., and Zaccai, G. (1992) *Adv. Protein Chem. 43*, 1−62.
21. Eisenberg, H (1995) *Arch. Biochem. Biophys. 318*, 1−5.
22. Dym, O., Mevarech, M., and Sussman, J. L. (1995) *Science 267*, 1344−1346.
23. Frolow, F., Harel, M., Sussman, J. L., Mevarech, M., and Shoham, M. (1996) *Nat. Struct. Biol. 3*, 452−458.
24. Zaccai, G., Cendrin, F., Haik, Y., Borochov, N., and Eisenberg, H. (1989) *J. Mol. Biol. 208*, 491−500.
25. Bonnete, F., Ebel, C., Zaccai, G., and Eisenberg, H. (1993) *J. Chem. Soc., Faraday Trans. 89*, 2659−2666.
26. Bonnete, F., Madern, D., and Zaccai, G. (1994) *J. Mol. Biol. 244*, 436−447.
27. Madern, D., and Zaccai, G. (1997) *Eur. J. Biochem. 249*, 607−611.
28. Richard, S. B., Madern, D., Gracin, E., and Zaccai, G. (2000) *Biochemistry 39*, 992−1000.
29. Pieper, U., Kapadia, G., Mevarech, M., and Herzberg, O. (1998) *Structure 6*, 75−88.
30. Kerscher, L., and Oesterhelt, D. (1976) *FEBS Lett. 67*, 320−322.
31. Kerscher, L., Oesterhelt, D., Cammack, R., and Hall, D. O. (1976) *Eur. J. Biochem. 71*, 101−107.
32. Pfeifer, F. Griffig, J., and Oesterhelt, D. (1993) *Mol. Gen. Genet. 239*, 66−71.
33. Hase, T., Wakbayashi, S., Matsubara, H., Kerscher, L., Oesterhelt, D., Rao, K. K., and Hall, D. O. (1977) *FEBS Lett. 77*, 308−310.
34. Bandyopadhyay, A. K., and Sonawat, H. M. (2000) *Biophys. J. 79*, 501−510.
35. Periasamy, N., Doraiswamy, S., Maiya, G. B., and Venkataraman, B. J. (1988*) J. Chem. Phys. 88*, 1638−1651.
36. Bevington, P. R. (1969) in *Data reduction and error analysis for the physical sciences*, McGraw-Hill, New York.
37. Swaminathan, R., Periasamy, N., Udgaonkar, J. B., and Krishnamoorthy, G. (1994b) *J. Phys. Chem. 98*, 9270−9278.
38. Eftink, M. R., and Ghiron, C. A. (1976) *Biochemistry 15*, 672−680.
39. Eftink, M. R., and Ghiron, C. A. (1981) *Anal. Biochem. 114*, 199−227.
40. Beechem, J. M., and Brand, L. (1985) *Annu. Rev. Biochem. 54*, 43−71.
41. Swaminathan, R., Nath, U., Udgaonkar, J. B., Periasamy, N., and Krishnamoorthy, G. (1996) *Biochemistry 35*, 9150−9157.
42. Cantor, C. R., and Schimmel, P. R. (1980) in *Biophysical Chemistry Part 2, Techniques for the study of biological structure and function* (Freeman, W. H., Ed.) San Francisco.
43. Britton, K. L., Stillman, T. J., Yip, K. S. P., Forterre, P., Engel, P. C., and Rice D. W. (1998) *J. Biol. Chem. 273*, 9023−9030.
44. Baxter, R. M. (1959) *Can. J. Microbiol. 5*, 47−57.
45. Kauzman, W. (1959) *Adv. Proteins Chem. 14*, 1−63.
46. Dill, K. A. (1990) *Biochemistry 29*, 7134−7155.
47. Krishnan, G., and Altekar, W. (1993) *Biochemistry 32*, 791−798.
48. Swaminathan, R., Krishnamoorthy, G., and Periasamy, N. (1994) *Biophys. J. 67*, 2013−2023.
49. Bhaumik, S. R., and Sonawat, H. M. (1999) *Physiol. Chem. Phys. Med. NMR 31*, 1−8.
50. Kulinski, T., Visser, A. J. W. G., O'Kane, D. J., and Lee, J. (1987) *Biochemistry 26*, 540−549.
51. Eftink, M. R., Gryczynski, I., Wiczk, W., Laczko, G., and Lakowicz, J. R. (1991) *Biochemistry 30*, 8945−8953.
52. Atkins, W. M., Stayton, P. S., and Villafranca, J. J. (1991) *Biochemistry 30*, 3406−3416.
53. Chabbert, M., Hillen, W., Hansen, D., Takahashi, M., and Bousquet, J. A. (1992) *Biochemistry 31*, 1951−1960.
54. Elcock, A. H., and McComman, J. A. (1998) *J. Mol. Biol. 280*, 731−748.
55. Werber, M. M., and Mevarech, M. (1978) *Arch. Biochem. Biophys. 187*, 447−456.
56. Jaenicke, R. (1981) *Annu. Rev. Biophys. Bioeng. 10*, 1−67.
57. Lanyi, J. K., and Stevenson, J. (1970) *J. Biol. Chem. 245*, 4074−4080.
58. Johnson, M. L. (1997) *Methods Enzymol. 278*, 570−583.
59. Chatelet, C., and Meyer, J. (1999) *J. Biol. Inorg. Chem. 4*, 311−317.
60. Meyer, J., Bruschi, M. H., Bonicel, J. J., and Bovier-Lapierre, G. E. (1986) *Biochemistry 25*, 6054−6061.
61. Ebel, C., Faou, P., Kernel, B., and Zaccai, G. (1999) *Biochemistry 38*, 9039−9047.

BI001614J